RESEARCH ARTICLE | JULY 25 2019

Design of efficient stamped mirror facets using topography optimisation

Nicholas Rumsey-Hill; Johannes Pottas; Joe Coventry

AIP Conf. Proc. 2126, 030048 (2019)
https://doi.org/10.1063/1.5117560

Design of Efficient Stamped Mirror Facets Using Topography Optimisation

Nicholas Rumsey-Hill[1, b)], Johannes Pottas[1, c)], and Joe Coventry[1, a)]

[1]*Research School of Engineering, Building 35A, Australian National University, Canberra, ACT 2601, Australia*

[a)]Corresponding author: joe.coventry@anu.edu.au
[b)]nicrumseyhill@gmail.com
[c)]johannes.pottas@anu.edu.au

Abstract. Significant cost reduction is required to improve the competitiveness of concentrating solar power. Heliostats make up a significant proportion of the capital cost of solar tower plants, with low-cost, high-performance designs required to meet levelised cost of energy targets. Lightweight stamped mirror facets are seen in leading commercial solar tower plants, with low manufacturing costs and high optical performance. Here, topography optimisation is investigated as a tool for designing lighter and structurally efficient stiffening bead patterns for stamped mirror facets. A case study is presented demonstrating topography optimisation as a promising tool for facet design, with tailored optimisation approaches incorporating wind and gravity load cases, manufacturing constraints, and combined optical-structural objectives. A range of concepts were generated, and their performance assessed to develop a design framework for high-performance supports. Wind loads in the stow position were found to influence and limit weight reduction more than gravity loads during operation. For the various concepts generated by optimisation, a common geometric feature was clearly-defined radial beads from the mounting points to a peripheral bead, driven by the need to overcome high bending stresses. Prototyping stamped structures is typically expensive. A low-cost and accessible rapid-prototyping method for stamped facets was developed using incremental sheet forming. A framework is presented for fabricating facets incorporating optimised supports, with photogrammetry and deflection tests enabling rapid assessment and structural modelling validation.

INTRODUCTION

The levelised cost of energy (LCOE) of concentrating solar power (CSP) must be reduced to be competitive with other energy generation technologies. This can be achieved by increasing plant efficiency or reducing life-cycle cost. Heliostats make up around 30-40% of the capital cost of tower CSP plants, with low-cost, high performance designs required to meet LCOE targets, such as the U.S. Department of Energy Sunshot goal of 0.06 USD/kWh [1]. Heliostat costs have fallen from around 150-200 USD/m^2 in 2013 [2] to an estimated 100-140 USD/m^2 [3], but significant further cost reduction is necessary to achieve the 75 USD/m^2 Sunshot target. Stamped mirror facets, comprising a glass mirror directly attached to a stamped sheet metal backing, have been deployed successfully at several large-scale and cost-competitive commercial projects, e.g. Gemasolar, Crescent Dunes, and Noor III.

Stamping is attractive as a low-cost and scalable manufacturing method, enabling simple fabrication of the support structure of mirror facets. The mirror and support are bonded together on a mould to fix the desired curvature. Stamped facets efficiently use thin sheet metal to form a high-stiffness geometry. This constrains mirror deformation to achieve high optical accuracy. Selected commercial designs and their key features are shown in Fig. 1a. The designs of each of these stamped facets have similar features, with trough-shaped stiffening beads connecting mounting points to perimeter reinforcement, and cut-out areas which reduce weight (Fig. 2b). Flexible adhesive withstands differential expansion between the steel and glass [4]. Stiffening geometry varies within the stamping to efficiently distribute reinforcement where needed, with various patterns seen commercially. Facets attach to a secondary support structure of box beams and trusses at four points to distribute loads throughout the stamping, which also enables canting facets relative to the planar secondary structure [5]. This reduces the dimensional tolerance required of support structures for

SolarPACES 2018
AIP Conf. Proc. 2126, 030048-1–030048-9; https://doi.org/10.1063/1.5117560
Published by AIP Publishing. 978-0-7354-1866-0/$30.00

lower costs. SolarReserve and Sener heliostats use an array of 1.5 m x 2.1 m facets with 20-50 mm bead depths, including a narrower perimeter bead.

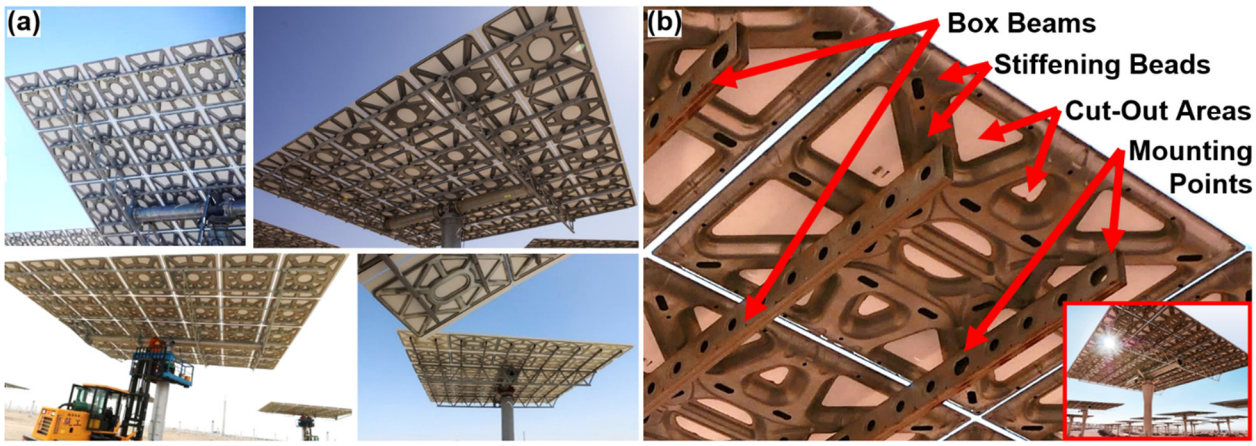

FIGURE 1. (a) Commercial multi-facet heliostats with stamped facets. Clockwise from top left; Crescent Dunes [6], Gemasolar [7], Dunhuang [8], and Suncan CSP plants [9]. (b) NOOR III heliostat incorporating stamped mirror supports [10].

Aggressive cost targets for widespread adoption of CSP necessitate innovative design approaches to reduce material usage and manufacturing cost of heliostats while maintaining shape accuracy and survivability during extreme wind. This requires mirror facet designs that efficiently distribute support material for high stiffness and low weight. The Kolb et al. analysis of the 4th generation ATS heliostat revealed simple steel components and mirrors accounted for 63% and 24% of the mass respectively [11]. Using bulk material costs, a minimum possible cost of 70 USD/m^2 was estimated in 2007 dollars, equivalent to 85 USD/m^2 today. This ignores assembly, installation costs, and components such as drives, yet still exceeds the Sunshot target of 75 USD/m^2. State-of-the-art heliostats employed at SolarReserve and Noor III plants retain the 'T-shape' and faceted structure analysed by Kolb. Modern heliostats are likely to have similar cost breakdowns, and solely increasing manufacturing volume cannot provide the necessary cost reduction to meet targets. Research is needed to develop designs with reduced material usage, that also employ high-volume manufacturing techniques to reduce other costs. For stamped facets, structural optimisation is a viable approach to reducing the specific mass of heliostats.

This work investigates the use of a shape optimisation method known as Topography Optimisation (TO), to efficiently incorporate stiffening beads into the sheet metal backing, improve structural performance, and minimise material use of stamped mirror facets. Prototyping stamped structures at low volume is typically prohibitively expensive [12]. Here, Incremental Sheet Forming (ISF) is demonstrated as a low-cost method to prototype stamped structures, where a typical Computer-Numerically-Controlled (CNC) mill is used to produce sheet metal parts through a process of gradual localised deformation. This allows rapid feedback on the efficacy of the TO method.

TOPOGRAPHY OPTIMISATION

Description

TO is a class of shape optimisation for shell structures, with important applications as a concept generation tool for designing stiffening bead patterns in sheet material [13]. TO is regularly applied in industries which benefit from weight reduction, such as stamped automotive components [14,15]. In this study, TO is investigated as a design tool for mass-efficient stamped mirror supports.TO can be applied using Finite-Element Modelling (FEM) to any structure meshed using shell-type elements, with boundary conditions and loads applied for the corresponding static analysis. GENESIS Design Studio (GDS), the software employed in this work, automatically generates perturbation vectors that point where shell nodes can move to, based on objectives such as element stress or angular displacement [13]. Optimisation progresses in cycles by assessing the sensitivity of the objective to allowed geometry changes, re-distributing material to where it has the greatest impact until convergence is reached.

TO effectively treats the displacement of shell nodes as design variables, iteratively modifying them to achieve specified design objectives. Geometric rules can be incorporated that reflect the manufacturing constraints of stamping including stamping direction, depth, and wall angles. Other parameters govern how the optimisation progresses from a geometric and mathematical perspective, such as limiting the area fraction of reinforcement. Objectives can be applied as weighted combinations of FEM responses, such as minimising displacement in response to a load case, or constraints such as maintaining stresses below failure. For stamped mirror facet supports, TO objectives should ideally result in a material distribution that makes the most efficient use of the strength of a given amount of material. In the ideal structure, stresses are evenly distributed throughout the structure. This produces the stiffest possible structure for a fixed amount of material while obeying the geometric constraints.

Mirror Facet Case Study

The applicability of TO for stamped support design was investigated with a 2.4 m x 1.5 m facet as a case study. The facet is supported at two 75 mm square mounting pads located 825 mm apart on the horizontal axis of the facet. The TO technique could equally be applied to other mounting arrangements, such as the more typical four pad mounts seen in commercial heliostat fields (e.g. Fig. 1). Optimisation was performed on a FEM model mirror facet of 20 mm shell elements shown in Fig. 2, assuming a static linear response. The layup consists of an initially planar stamped steel support sheet and a glass-on-metal laminate (GOML) of 1.0 mm glass and 0.4 mm steel. A glue constraint bonds the GOML internally, and a separate constraint glues the support sheet to the GOML only at adjacent areas. The optimisation modifies the designable area (labelled in Fig. 2b) of the support as it progresses. A fixed displacement constraint was applied to mounting locations (also labelled in Fig. 2b), which extended from the mirror plane to the desired bead depth. These areas cannot be modified by the optimisation.

Pfahl et al. [16] suggest that the most important structural criteria for the design of heliostats are withstanding storms in stow position and low deformation due to gravity during operation, and that the impact of wind loads on performance during operation is minor. This latter assertion is supported by other work based on experimental [17] and validated FEM approaches [18,19]. These criteria embody two approaches to LCOE reduction: reducing optical losses with high-stiffness designs; and reducing structural steel required to withstand maximum winds in stow. To verify that the greatest structural forces occur when a heliostat is stowed during severe winds, the method outlined by Peterka et al. [20] for estimating resultant wind loadings was employed. Based on SunShot design targets [21], it was assumed that the heliostat operates in wind speeds up to 15 m/s and must withstand up to 38 m/s winds in stow. At these rated wind speeds, loads on the support structure in stow were confirmed to dominate those experienced during operation.

Accordingly, two load cases were investigated for optimisation. First, an operating case with the facet tilted at 25° to the horizontal (power-weighted average for Pretoria [22]) with a gravity load applied. Second, a horizontal stow case with gravity and a non-uniform wind pressure distribution for a 38 m/s wind. Figure 2c shows the pressure distribution used, which is based on data from wind tunnel experiments on a square heliostat scale model at the University of Adelaide [23]. In the present work, the square pressure distribution was elongated to fit the rectangular facet used for the case study. This results in two pressure distributions representing distinct loads with the facet's short and long edges facing into the wind, and these were applied as equally-weighted loads for the stow case.

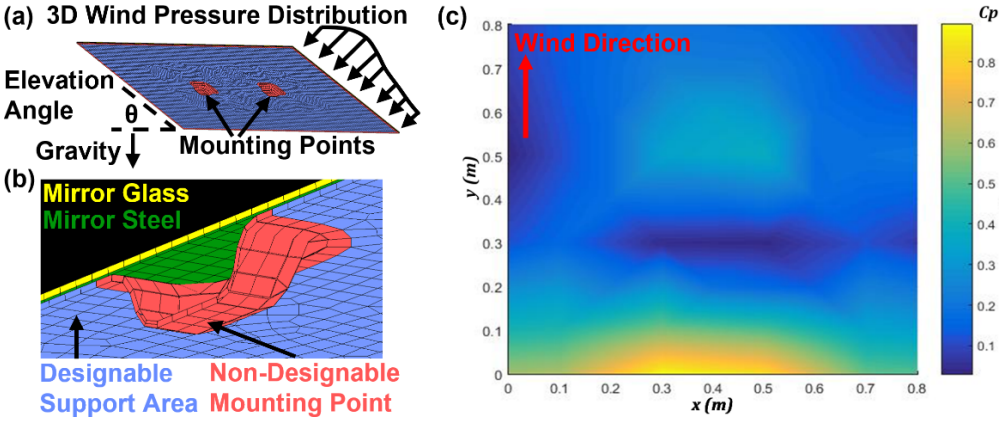

FIGURE 2. (a) Finite-element model of the facet pre-optimisation showing fixed mounting points and loads. (b) Section view showing FEM groups. (c) Peak pressure coefficient distribution measured from scale wind-tunnel tests of a stowed heliostat [23].

Analysis Method and Results

The impact of various objective functions on mirror deflection was assessed. These provide TO software with a numerical target for design performance. Ideal TO for stamped facets would simultaneously minimise mirror shape error (i.e. the RMS average of angular deviations of the mirror normal vectors due to change in surface shape under load) and support mass to withstand wind loads for the operational and stow cases respectively. However, the case study was limited by the software used. GDS cannot remove support material to form cut-out areas during optimisation to reduce mass. Another limitation was that it cannot minimise area-average values of outputs such as stress or displacement. Objectives were trialed to minimise displacement at selected points, which resulted in poor designs with large areas of mirror unsupported and high displacements. More complex objective functions, ideally shape error, were not able to be implemented within the software. It was found that the lowest average mirror displacement values were achieved by minimising strain energy in the mirror laminate and stamped support with equal weighting, and thus strain energy was selected as the objective function. Fig. 3a shows a typical facet displacement under a gravity load after optimisation with this objective, with deformation distributed across the facet. Unfortunately, although mirror displacement was minimised using strain energy, it was found to be a relatively poor proxy for other objectives of interest: shape error (calculated in post-processing) and stress uniformity within the support. For example, localised bending around the mounting points can yield low strain energy, but also poor optical performance and stress concentrations in the support.

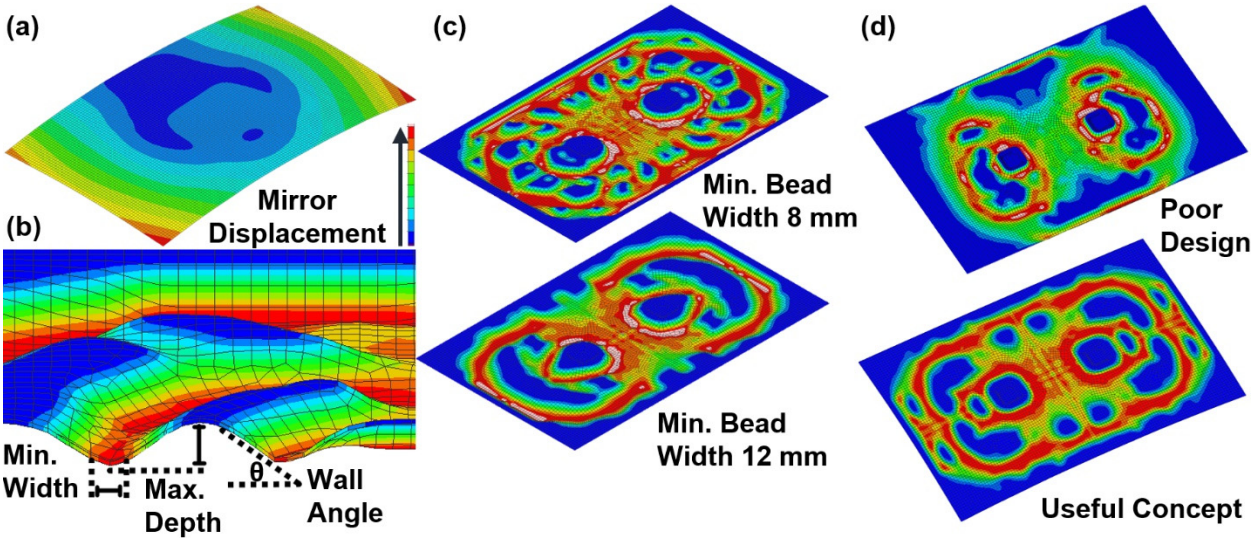

FIGURE 3. (a) Typical facet displacement plot resulting from the gravity load. (b) Close-up of optimisation output with key parameters labelled. (c) Minimum width strongly impacts bead pattern complexity. (d) Shape change plots of poorly-defined optimisation output (top), and a better shape with clearly-defined stiffening beads (bottom). Red areas indicate maximum depth.

In GDS, some geometric parameters can be used to limit the maximum bead depth, wall angles, and minimum bead width. These were set to 50 mm, 70°, and 60 mm respectively. Ideally, bead geometry could be constrained to incorporate stamping design rules for the greatest specific stiffness. These are seen in commercial stamped facets, with consistent steep wall angles as well as bead depth and width. However, these are only partially controlled in GDS (Fig. 3b), limited to upper bounds on wall angle and bead depth, and a lower bound on bead width. Instead, irregular geometry of varying bead depth and wall angles is typical (Fig. 3d), which is impractical to manufacture and sub-optimal as a high-stiffness design. As a result, many support concepts generated from the optimisation were not practicable. Many had irregular beads or large areas with the mirror unsupported, and ignored stamping guidelines.

Various mathematical parameters for the optimisation were investigated, such as move limits, bead fraction limits, and initial displacements. These resulted in distinct changes in the optimised designs by governing how the algorithm progresses between design cycles. Decreasing minimum bead width allows finer reinforcement patterns to develop (Fig. 3c), which generally exhibited lower average mirror displacements under gravity but would require thinner sheet metal considering they have less removable area. Symmetry constraints were useful to force generic designs optimised from asymmetric pressure distributions. Overall, careful choice of parameters can yield useful optimised concepts

(Fig. 3d). For the operational load case, average mirror deflection under gravity was used to compare performance of optimised shapes, as a proxy for shape error which could not be measured in GDS. For the wind load case, maximum stress in the support would ideally indicate performance, but the use of a coarse mesh and resulting stress singularities around mounting points decreased the reliability of this metric.

Figure. 4 shows selected, representative TO output from the study. Shapes (a) and (b) resulted from the operational case. The gravity load is evenly distributed across the facet area, which results in fine reinforcement structures. Before post-processing, shape (a) resulted in the lowest average mirror displacement of those optimised with the operational load case. Large areas with poorly defined reinforcement are shown in green, highlighting the need for precise geometry control in TO software. These areas impact stiffness performance, are impractical for stamped facets, and were ignored during the post-processing steps described below. Overall, stiffening reinforcement was generated to connect supported areas in the centre to the distributed load. TO can reveal counter-intuitive designs, and the trends in optimised shapes provide evidence for similar attributes seen in commercial stamped facets.

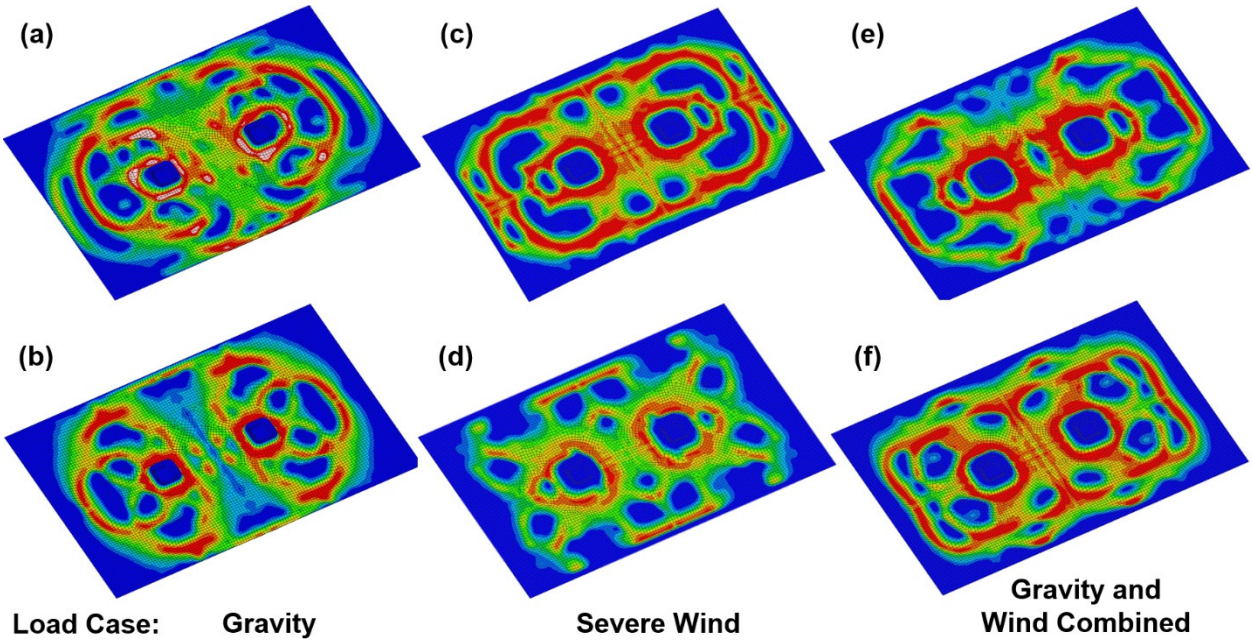

FIGURE 4. Selected optimisation output resulting from three different load cases. Shapes (a) and (b) resulted from the operational load case with gravity only, (c) and (d) from the stow load case with a wind load, while (e) and (f) were produced from an equally-weighted combination of both.

Shapes (c) and (d) resulted from the stow case. These are presented as examples of designs that resulted in the lowest and highest maximum wind load stresses after post-processing respectively. High wind pressure load at the leading edge of the mirror facet (refer to the pressure distribution in Fig. 2c) induces a high bending moment on the facet. The optimisation responds with stiffer reinforcement along primary mirror axes, as well as deeper beads in the perimeter regions. Shapes (e) and (f) were optimised from the equally-weighted combination of the two load cases, with geometric features between those optimised solely for gravity or wind. Compared to those optimised for gravity, these shapes exhibited less intricate reinforcement, but not as simple or clearly defined as produced by the wind load. This is exemplified in shape (f), with geometry and hence expected performance between that of (a) and (c).

Post Processing and Performance Assessment

The resulting geometry from the TO required adjustment to meet manufacturing constraints of metal stamping, including the wall angle and bead depth, as well as removing non-designed flat areas shown in blue in Fig. 4. Guidelines for support geometry were developed, informed by existing designs as well as stamping and ISF constraints (Fig. 5a). A 50 mm bead depth for high specific stiffness, and 25 mm attachment flanges for mirror adhesion, were estimated from commercial stamped facets. A 70° wall angle and filleted vertices ensured compatibility with stamping

and ISF for prototyping [24]. Two examples of post-processed support structures are shown in Fig. 5b. FEM was then used to find the shape error under gravity and maximum support structure stress under severe wind. A parametric study of these variables with varying support thicknesses was performed. This found the minimum mass required to survive severe winds and the corresponding operational shape error for each concept, labelled on Fig. 5b. Failure occurs around the mounting points due to stress concentration, requiring compliant attachment methods, such as washers and box-beams seen in the NOOR III heliostat [5,10].

Wind-induced support stress was found to effectively limit design, with low shape errors of 0.1-0.3 mrad at the minimum thicknesses to prevent failure seen in all concepts. Reinforcement following simple load paths from the mounting points to the facet perimeter performed best. This is seen in shape C, which withstood maximum loads at the lowest weight of all concepts. Shape A has an indirect load path, concentrating bending stress where beads meet, requiring a greater thickness to survive. Continuous reinforcement around the facet perimeter is crucial for maximising stiffness against wind loads and is seen in all commercial designs.

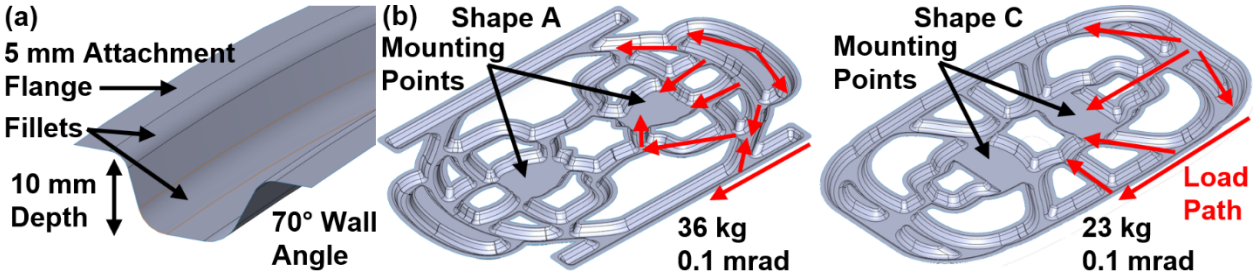

FIGURE 5. (a) Reinforcing bead geometry incorporating stamping and ISF design rules. (b) Post-processed supports based on shapes in Fig. 4a and Fig. 4c, with minimum mass to survive maximum wind loads and corresponding operational shape error.

PROTOTYPING USING INCREMENTAL SHEET FORMING

Stamping is a low-cost manufacturing method at high volume, but impractical for short-run prototyping due to long processing times, expensive tooling, and heavy machinery [12]. ISF was investigated as a low-cost solution for approximating stamped facet supports, which can be fabricated into prototype facets for analysis. ISF has proven applications in prototyping and low-volume manufacturing of similarly complex parts [25]. A CNC mill with hemispherical tool gradually deforms a clamped metal sheet into the desired geometry through continuous localised deformation, enabling rapid prototyping of stamped parts at significantly lower cost. Compared to stamping, ISF is accessible, fast, requires no specialised equipment, and is limited only by the size of CNC mill. Disadvantages include poor geometric tolerances of ± 1 to ± 4 mm, significant wall thinning, and the requirement for multiple-pass ISF for large strains or steep wall angles [25].

A method for producing functional 480 mm x 300 mm 1:5 scale prototype facets was developed using Two-Point Incremental Forming (TPIF). Here, the worksheet is clamped over a 3D-routed Medium-Density Fibreboard (MDF) die, which enables forming of complex geometries (Fig. 6a). Worksheet failure from localised thinning is common in ISF, and significant thinning occurs in steep walls. This is not expected to appreciably reduce facet stiffness as material furthest from the neutral axis of bending dominates stiffness. A reliable process for prototype stamping design that avoids part failure was developed, with key geometric features shown in Fig. 5. Aluminium AA-6061 1 mm sheet was cut to match the 500 mm x 320 mm die, and evenly clamped at the perimeter with gear oil applied (Fig. 6b). Aluminium was chosen for its improved formability over steel, without unacceptably compromising the prototyping objectives of proof-of-concept, validation of FEM, and identification of potential manufacturing issues. ISF processes are equally applicable to steel with minor process differences [25]. The support is formed into the die, alternating between tracing wall contours and incremental downward movements (Fig. 6c). CNC-milling is then used to cut the support from the sheet, with a 5 mm offset forming attachment flanges (Fig. 6d).

Maximum forming depths are difficult to predict for ISF. A 10 mm depth was chosen after several trials, equivalent to 50 mm at full scale. Sharp curvatures and deep forming should be avoided to prevent thinning failure. The prototypes featured 6 mm fillets on all internal edges corresponding to the ISF tool diameter, which limits curvature. Minor warping is inevitable due to residual stresses, as is spring-back in the attachment flanges. Prototype supports were manually de-burred and cleaned after forming. The TPIF formed aluminium supports were bonded to a GOML layup of 0.4 mm galvanised steel and 1 mm mirror glass. A vacuum-bagging process over a 30 m radius spherical

mould was used to compress the layup during bonding (Fig. 6f). Epoxy adhesive was used, with best results achieved with low-viscosity glue and sanded attachment flanges.

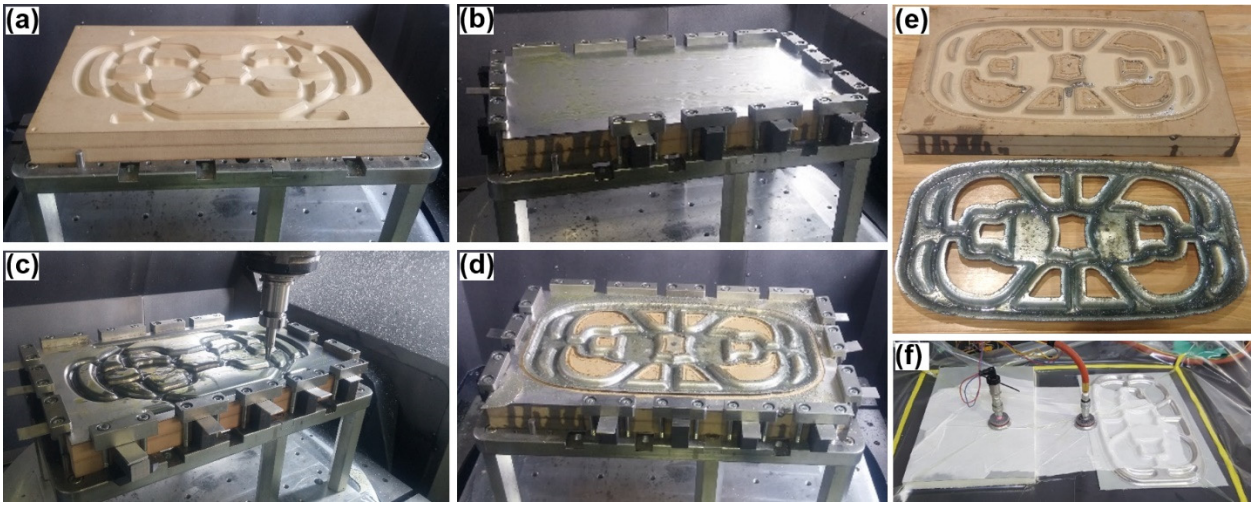

FIGURE 6. The prototyping process: (a) 3D-routed MDF die of the support shape is (b) clamped underneath a 1 mm aluminium sheet in a CNC mill. (c) A hemispherical tool incrementally forms the support shape, before (d) the support is cut from the metal and (e) removed from the mould. (f) The scale facet is then vacuum-formed over a spherical mould.

Single-point displacement tests on these prototypes were used to validate the accuracy of FEM results, with the modelling systematically under-predicting displacement by 30%. The discrepancy is attributed to differences in the manufactured geometry due to wall-thinning and warping. Photogrammetry was used to measure mirror curvature of the facets and is a useful technique for identifying manufacturing issues and assessing optical quality. Figure 7 shows the measured shape and residual plot of a prototype of concept A in Fig. 5a. Shape accuracy was best in the centre and decreased towards the edges of the facet due to edge effects. Spring-back in the support flanges resulted in the facet having a steeper curvature than the mould.

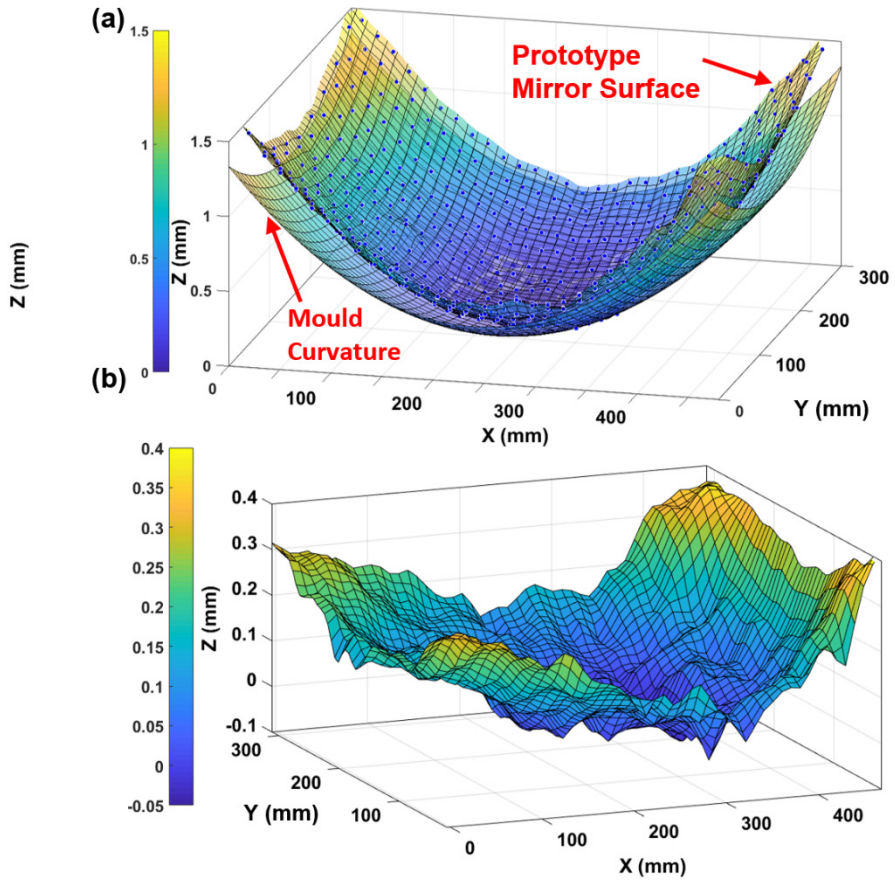

FIGURE 7. Photogrammetry measurement of the prototype facet based on shape C, with (a) the surface curvature compared to the mould, and (b) the residual plot of deviation from the mould.

CONCLUSION

Topography optimisation is a promising tool for the design of lightweight stamped mirror facets. A tailored optimisation approach for generating mass-efficient concepts was developed with a case study, enabled by implementing load cases, objectives, and manufacturing constraints to improve optical-structural performance. In this study, software constraints limited the choice of the objective function for the optimisation. Ideally this would jointly minimise mass, distribute stress as evenly as possible and minimise shape error. Nonetheless, useful concepts were produced from a strain energy objective. Other TO software capabilities identified as important for future work on mirror facets are control of bead geometry to implement stamping design guidelines, as well as the ability to remove featureless areas as part of the optimisation. With this, the shape error and support stress responses could be more easily compared in-situ, increasing confidence in design selection.

Despite these limitations, the wide range of support geometries generated and assessed provided insight for stamped facet design. Optimised supports with stiffening beads directly linking mounting locations with perimeter reinforcement best distributed stresses across the structure, which is important for weight reduction. Concepts optimised for a severe wind load showed the best performance, with distinct bead structures that maximised facet stiffness compared to the finer structures optimised for the evenly-distributed gravity load. Survival during severe winds limits weight reduction, with low gravity-induced shape errors observed at minimum thicknesses to prevent failure. These results suggest optimising for minimum weight and evenly-distributed support stress during severe winds is a promising approach for facet design.

Incremental sheet forming was used to develop a rapid-prototyping method which is accessible and low-cost. The ISF process imposes additional geometry constraints, exhibits wall-thinning, and has lower dimensional accuracy compared to stamping. Despite this, incremental forming may offer a low-cost solution for pilot-scale plants or small-run heliostat installations.

REFERENCES

1. M. Mehos, C. Turchi, J. Jorgenson, P. Denholm, C. Ho, and K. Armijo, *On the Path to SunShot: Advancing Concentrating Solar Power Technology, Performance, and Dispatchability* (National Renewable Energy Laboratory, Golden, CO, 2016).
2. J. Coventry, J. Campbell, Y.P. Xue, C. Hall, J.S. Kim, J. Pye, G. Burgess, D. Lewis, G. Nathan, M. Arjomandi, W. Stein, M. Blanco, J. Barry, M. Doolan, W. Lipinski, and A. Beath, *Heliostat Cost Down Scoping Study-Final Report* (Australian Solar Thermal Research Initiative, 2016).
3. H. Hashem, < http://newenergyupdate.com/csp-today/csp-tower-installation-costs-drop-heliostat-innovations-pre-assembly> (2017).
4. J.M.L. Pérez, U.S Patent No. 8,567,970 B2 (October 29 2013).
5. Nikon Metrology, <https://www.nikonmetrology.com/images/case-studies/sener-laser-radar-en.pdf> (2010).
6. SolarReserve, <https://www.solarreserve.com/en/global-projects/csp/crescent-dunes> (2018).
7. SENER, <http://www.ingenieriayconstruccion.sener/proyecto/gemasolar> (2018).
8. J. Zhang, <http://en.cspplaza.com/chinas-dunhuang-100mw-molten-salt-tower-csp-plant-has-completed-its-civil-work-on-may-17/> (2018).
9. China National Solar Thermal Alliance, < http://en.cnste.org/html/csp/2015/0914/165.html> (2015).
10. J. Walters, <http://cmimarseille.org/menacspkip/alphabet-soup-climate-finance-csp-waccs-unfccc/> (2018).
11. G.J. Kolb, S.A. Jones, M.W. Donnelly, D. Gorman, R. Thomas, R. Davenport, and R. Lumia, *Heliostat Cost Reduction Study* (Albuquerque, New Mexico, USA, 2007).
12. S. Kalpakijan, K. Vijai Sekar, and S. Schmid, "Sheet-Metal Forming Processes and Equipment" in Manufacturing Engineering and Technology (Pearson, 2009) pp. 432.
13. J.P. Leiva, in 5th World Congr. Struct. Multidiscip. Optim. Venice, Italy (2003).
14. D. Schneider, and T. Erney, in OptiCON 2000 Conference Proceedings (2000).
15. W. Choi, C. Huang, J. Kim, and G. Park, in 11th World Congr. Struct. Multidiscip. Optim. (2015).
16. A. Pfahl, J. Coventry, M. Röger, F. Wolfertstetter, J.F. Vásquez-Arango, F. Gross, M. Arjomandi, P. Schwarzbözl, M. Geiger, and P. Liedke, Sol. Energy 152, 3 (2017).
17. J.W. Strachan and R.M. Houser, *Testing and Evaluation of Large-Area Heliostats for Solar Thermal Applications* (Sandia National Labs., Albuquerque, NM, 1993).
18. E. Teufel, R. Buck, A. Pfahl, G. Böing, and J. Kunert, in SolarPaces Conf. (2008).
19. F. Vásquez, "Dynamic Wind Loads on Heliostats", Ph.D. thesis RWTH Aachen University, 2016.
20. J. Peterka and R. Derickson, Rep. SAND 92–7009. Sandia Natl. Lab. (1992).
21. M. Mehos, C. Turchi, J. Vidal, M. Wagner, Z. Ma, C. Ho, W. Kolb, C. Andraka, and A. Kruizenga, *Concentrating Solar Power Gen3 Demonstration Roadmap* (National Renewable Energy Laboratory, Golden, CO, 2017).
22. R. Buck, A. Pfahl, and T.H. Roos, in Proc. 1st South. African Sol. Energy Conf. (2012).
23. M.J. Emes, M. Arjomandi, F. Ghanadi, and R.M. Kelso, Sol. Energy 157, 284 (2017).
24. D. Adams and J. Jeswiet, Proc. Inst. Mech. Eng. Part B J. Eng. Manuf. 229, 754 (2015).
25. D. Afonso, R. Alves de Sousa, and R. Torcato, Int. J. Adv. Manuf. Technol. (2017).